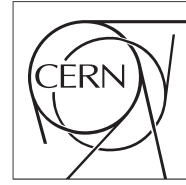**The Compact Muon Solenoid Experiment**

Conference Report

Mailing address: CMS CERN, CH-1211 GENEVA 23, Switzerland

20 November 2024 (v2, 22 November 2024)

Spectroscopy of beauty strange baryons at CMS

Kirill Ivanov for the CMS Collaboration

Abstract

Latest CMS results on spectroscopy of beauty strange baryons are reported, including new decay modes and studies of excited states. The analyses use pp collision data at 13 TeV.

Presented at *ICPPA-2024 7th International Conference on Particle Physics and Astrophysics*

Heavy flavour spectroscopy and properties at CMS

Kirill Ivanov on behalf of the CMS Collaboration[1, 2, *]

[1]*Moscow Institute of Physics and Technology, Institutsky lane 9, Dolgoprudny, Moscow region, 141700 Russia*
[2]*P. N. Lebedev Physical Institute of the Russian Academy of Sciences, Moscow, 119991 Russia*

Latest CMS results on spectroscopy of beauty strange baryons are reported, including new decay modes and studies of excited states. The analyses use pp collision data at 13 TeV.

I. INTRODUCTION

The Compact Muon Solenoid (CMS) Experiment [1] is one of the two general-purpose detectors at the CERN LHC and is designed to yield a wide range of potential physics outcomes. In particular, its exceptional muon system, remarkable particle transverse momentum resolution, and robust vertexing capabilities — including the ability to reconstruct cascades of displaced vertices — allow the CMS Collaboration to conduct state-of-the-art studies within the heavy flavour sector. One of the key advantages in this area is the opportunity to utilize the muons produced from charmonia decays (J/ψ and ψ(2S) mesons).

In this talk we discuss the results, based on studies of $\Xi_{\rm b}$ baryons at the CMS Experiment with the data sample collected in proton-proton collisions at $\sqrt{s}$ = 13 TeV in 2016–2018, corresponding to an integrated luminosity of 140 fb^{-1} [2, 3].

II. $\Xi_{\rm b}$ BARYON FAMILY

The $\Xi_{\rm b}$ baryon family are of isodoublet states composed of qsb quarks, where q represents an up or a down quark for the $\Xi_{\rm b}^0$ and $\Xi_{\rm b}^-$ states, respectively. Three such isodoublets are neither orbitally nor radially excited (the $\Xi_{\rm b}$ ground states with $J^P = 1/2^+$ and $j_{\rm qs} = 0$, $\Xi_{\rm b}'$ with $J^P = 1/2^+$ and $j_{\rm qs} = 1$, and $\Xi_{\rm b}^*$ with $J^P = 3/2^+$ and $j_{\rm qs} = 1$). Three of the states with $j_{\rm qs} = 1$ have been previously observed at the LHC by CMS [4] and LHCb [5, 6] via their $\Xi_{\rm b}^- \pi^+$ and $\Xi_{\rm b}^0 \pi^-$ decays. The fourth state, $\Xi_{\rm b}'^0$, is expected to be lighter than the $\Xi_{\rm b}^- \pi^+$ mass threshold, making a strong transition to $\Xi_{\rm b}^-$ kinematically impossible. The next prominent isodoublets, in analogy with the well-established excited $\Xi_{\rm c}$ baryons [7], are orbitally excited 1P-doublet of $\Xi_{\rm b}^{**}$ states with $J^P = 1/2^-$ (3/2$^-$) and expected to decay to $\Xi_{\rm b}'(\Xi_{\rm b}^*)\pi$, where $L = 1$ between the b quark and the ds diquark. The scheme of these isodoublets is provided in Fig. 1. Several more heavy $\Xi_{\rm b}$ resonances, supposed to be 1D excited states and 2S or a heavier 1P isodoublet states, have been also recently observed by the LHCb Collaboration [8–10].

The classification of different $\Xi_{\rm b}$ states and their strong decays is relatively straightforward, particularly for the discussed lightest excitations. Conversely, the description of the various weak decay modes of the ground-state baryons within the framework of heavy-quark effective theory (HQET) [11] presents a substantial theoretical challenge, resulting in less straightforward predictions of branching fractions to various final states. Measurements of the decays and properties of both ground and excited $\Xi_{\rm b}$ states provide crucial input to our comprehension of the complicated QCD mechanisms governing quark dynamics within hadrons.

III. EVENTS RECONSTRUCTION

In the present study we reconstruct the $\Xi_{\rm b}^-$ baryon ground state via two main decay modes: $\Xi_{\rm b}^- \to \psi \Xi^-$, followed by $\psi \to \mu^+ \mu^-$, where ψ stands for both J/ψ and ψ(2S) mesons, or $\Xi_{\rm b}^- \to$ J/$\psi \Lambda {\rm K}^-$. The pictorial schemes of the decay topologies are provided in Fig. 2.

The reconstruction process starts with the selection of two opposite-sign muons, which are significantly displaced from a pp collisions primary vertex (PV) with the additional requirement of dimuon invariant mass to be close to the world-average J/ψ or ψ(2S) mass [7]. Then a Λ hyperon candidate is selected using its decay $\Lambda \to p\pi^-$, formed as the detached vertex with two originating V-like tracks with a zero summed charge (V0). For the $\psi \Xi^-$ mode, an additional charged particle track with a pion mass assignment is then added, and it is fitted with a Λ pseudo-track into a common vertex, forming Ξ^- hyperon decay to $\Lambda \pi^-$. Finally, the $\Xi_{\rm b}^-$ candidates are obtained using the muons and Ξ^- particle in a kinematic vertex fit, which constrains the dimuon invariant mass to the world-average J/ψ or ψ(2S) meson mass [7]. For the $\Xi_{\rm b}^- \to \psi$(2S)Ξ^- mode we also reconstruct a chain with two additional pion tracks, corresponding to ψ(2S) $\to$ J/$\psi \pi^+ \pi^-$ decay. For the J/$\psi \Lambda {\rm K}^-$ mode, a kaon mass instead of a pion is assigned to the charged particle track, and the kinematic vertex fit to form $\Xi_{\rm b}^-$ candidates includes μ^+, μ^-, Λ, and kaon particles.

The selection criteria are optimized using the Punzi figure of merit [12] and require significant displacement of all secondary vertices from the primary vertex, alignment of the transverse momentum with the transverse displacement vector between the particles, $p_{\rm T}$ and η restrictions, and other requirements.
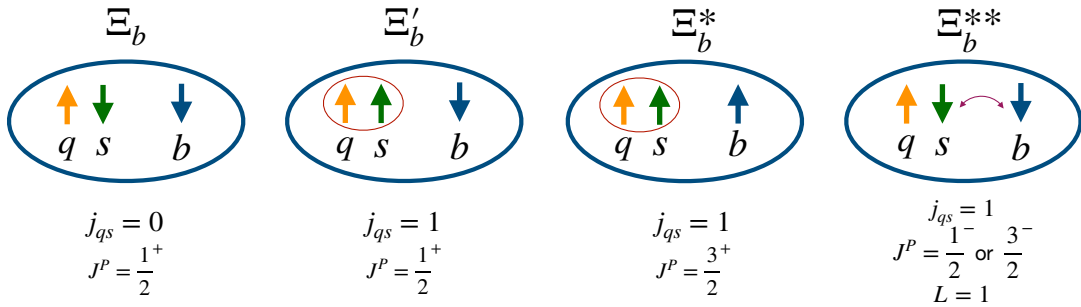
---

*Electronic address: kirill.ivanov@cern.ch

FIG. 1: Quark spin configurations for the lightest Ξ_b isodoublets, q corresponds to up and down quarks for Ξ_b^0 and Ξ_b^-, respectively [2].
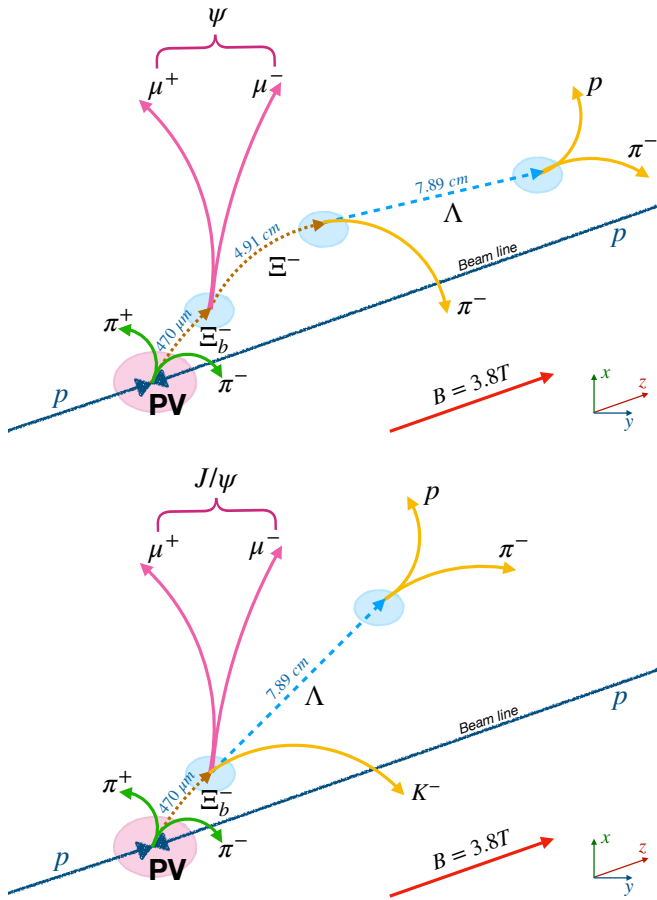

FIG. 2: The $\Xi_b(6100)^- \to \Xi_b^- \pi^+ \pi^-$ decay topology in which the Ξ_b^- baryon decays to $\psi \Xi^-$ with $\psi \to \mu^+ \mu^-$ (upper) or $J/\psi \Lambda K^-$ (lower), where ψ refers to the J/ψ and $\psi(2S)$ mesons [2].

IV. OBSERVATION OF THE $\Xi_b^- \to \psi(2S)\Xi^-$ DECAY

Figure 3 presents the invariant mass distributions for the $J/\psi \Xi^-$, $J/\psi \Lambda K^-$ and $\psi(2S)\Xi^-$ candidates, where the latter divided into the two modes of $\psi(2S)$ reconstruction: $\mu^+ \mu^-$ or $J/\psi \pi^+ \pi^-$. An unbinned extended maximum likelihood fit is performed on each of these distributions. The signal is described with a double Gaussian function with a common mean and the background is described with a first-order polynomial or an exponential function. The $J/\psi \Lambda K^-$ distribution also presents a contribution from the partially reconstructed $\Xi_b^- \to J/\psi \Sigma^0 K^-$ decay, where photon from $\Sigma^0 \to \Lambda \gamma$ decay is not detected. This contribution is taken into account by including an asymmetric Gaussian in the fit, with its shape parameters are fixed from MC simulation.

Statistical significance of the $\Xi_b^- \to \psi(2S)\Xi^-$ signal (never previously reported) is estimated with the likelihood ratio technique, comparing a signal-plus-background hypothesis versus a background-only hypothesis. The obtained value is well above 5 standard deviation, indicating the first observation of the new decay. We have also measured its branching fraction w.r.t. the normalization channel $\Xi_b^- \to J/\psi \Xi^-$:

$$
\begin{aligned}
R &= \frac{\mathcal{B}(\Xi_b^- \to \psi(2S)\Xi^-)}{\mathcal{B}(\Xi_b^- \to J/\psi \Xi^-)} = \frac{N(\Xi_b^- \to \psi(2S)\Xi^-)}{N(\Xi_b^- \to J/\psi \Xi^-)} \\
&\times \frac{\epsilon(\Xi_b^- \to J/\psi \Xi^-)}{\epsilon(\Xi_b^- \to \psi(2S)\Xi^-)} \frac{\mathcal{B}(J/\psi \to \mu^+ \mu^-)}{\mathcal{B}(\psi(2S) \to \mu^+ \mu^-)} \\
&= 0.84^{+0.21}_{-0.19}(\text{stat}) \pm 0.10(\text{syst}) \pm 0.02\,(\mathcal{B}),
\end{aligned}
\tag{1}
$$

where the last uncertainty is related with the to the uncertainties in the J/ψ and $\psi(2S)$ branching fractions. In this formula N and ϵ represent the measured number of signal events in data and the total efficiency from Monte Carlo (MC) simulation, respectively. The choice of the normalization channel is quite natural since it has identical topology and similar kinematic properties, allowing us to significanty reduce systematic uncertainties, related with muons and tracks reconstruction, in the measured ratio R.

The remaining systematic uncertainties includes variations of the signal and background models of the fit, the source related with the finite size of MC simulation samples, and accounting of the possible effects due to
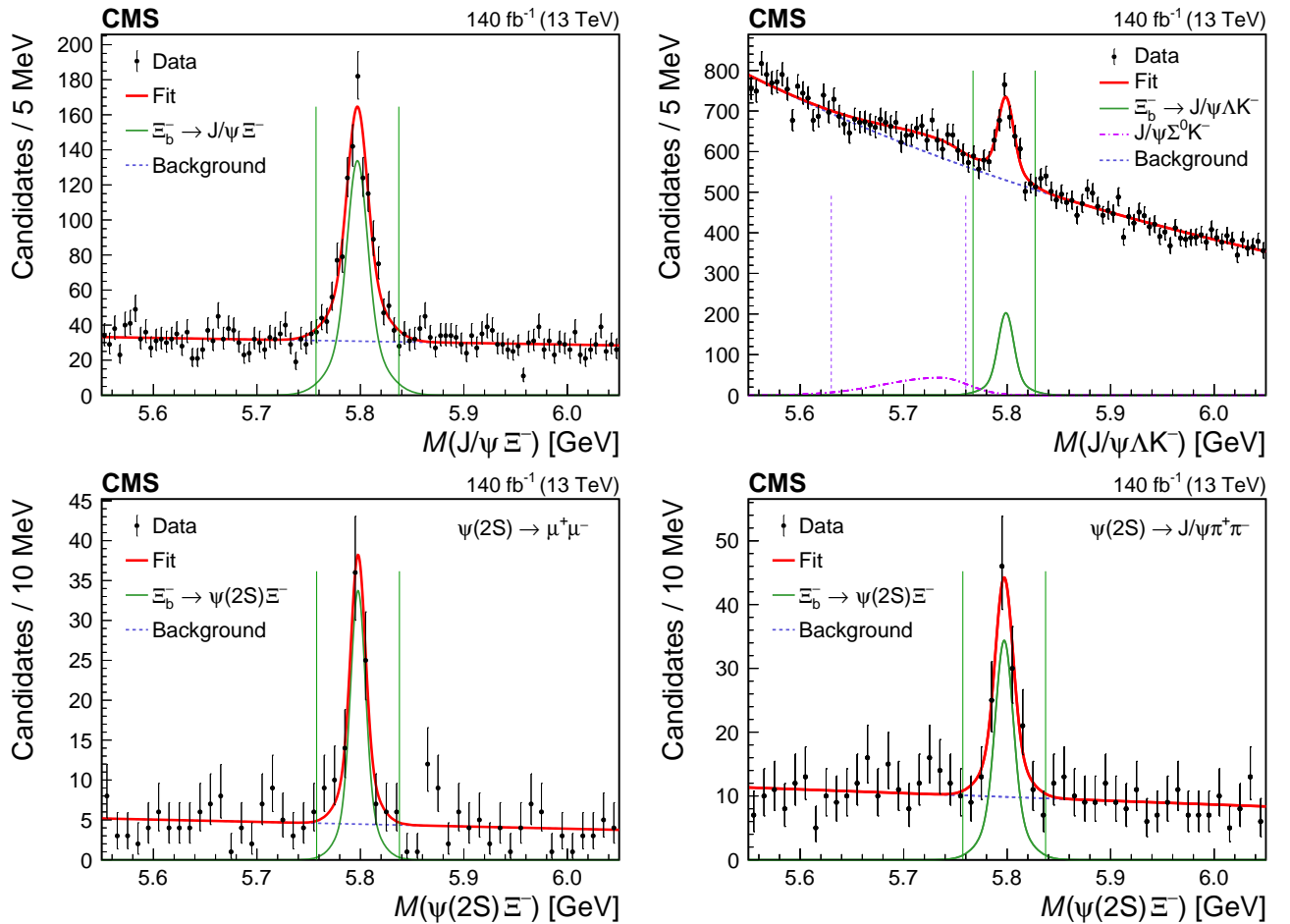
FIG. 3: Invariant mass distributions of the selected $J/\psi\Xi^-$ (upper left), $J/\psi\Lambda K^-$ (upper right), and $\psi(2S)\Xi^-$ [lower row, with $\psi(2S) \to \mu^+\mu^-$ (left) and $\psi(2S) \to J/\psi\pi^+\pi^-$ (right)] candidates, with superimposed fit results [3].

different trigger paths used for collecting events with J/ψ and $\psi(2S)$ mesons.

For the following studies of the $\Xi_b^-\pi^+$ and $\Xi_b^-\pi^+\pi^-$ systems, the selected Ξ_b^- candidates within the mass windows, shown in the Fig. 3 with green (purple) lines for the fully (partially) reconstructed events, are combined with a charged pion track (or two oppositely charged tracks), originating from the PV. In order to improve the detector resolution, we apply a dedicated procedure of PV kinematic refit, following the technique developed in Ref. [13].

V. STUDIES OF THE Ξ_b^{*0} BARYON

Figure 4 presents the distributions of the invariant mass difference variable, defined as $\Delta M = M(\Xi_b^-\pi^+) - M(\Xi_b^-) - m^{\mathrm{PDG}}(\pi^+)$, for the selected $\Xi_b^-\pi^+$ candidates separately for four channels of Ξ_b^- reconstruction. The ΔM variable allows us to subtract the Ξ_b^- mass resolution, resulting with significant improvement for possible signal sensitivity. We see a clear peak near the kinematic threshold in all 4 distributions, corresponding to

the known Ξ_b^{*0} resonance. To describe this signal, we use a relativistic Breit–Wigner function, convoluted with a Gaussian detector resolution, which shape is fixed with the values obtained in the MC simulation, while the background is described with a threshold function.

In order to measure the parameters of the Ξ_b^{*0} baryon, we use a simultaneous fit of all four channels, where the mass and natural width of the peak are shared parameters of the fit, while the mass resolutions, yields, and background parameters are different. The measured mass difference and natural width of the Ξ_b^{*0} state are $\Delta M(\Xi_b^{*0}) = 15.810 \pm 0.077(\mathrm{stat}) \pm 0.052(\mathrm{syst})\,\mathrm{MeV}$, $\Gamma(\Xi_b^{*0}) = 0.87^{+0.22}_{-0.20}(\mathrm{stat}) \pm 0.16(\mathrm{syst})\,\mathrm{MeV}$. The possible sources of the systematic uncertainties are the variations of the signal and background models, including the parameters of the Breit–Wigner function and detector resolution, variation of the fit range, and the contribution from the mass shift, observed in the MC simulation.

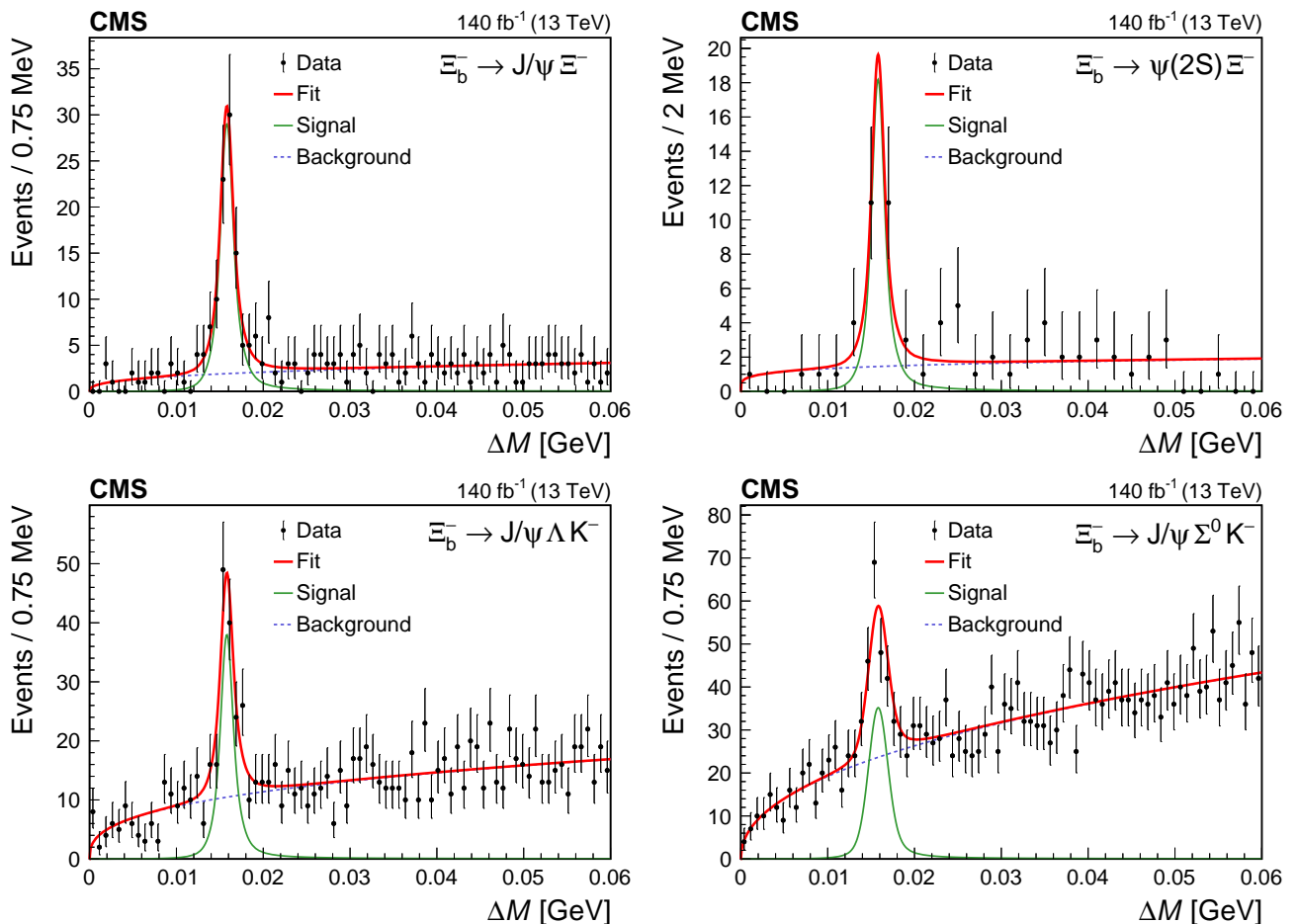We have also measured the ratio of the Ξ_b^{*0} to Ξ_b^- production:

FIG. 4: The mass difference ΔM distribution of the selected $\Xi_b^- \pi^+$ candidates for the decay channel labeled on each plot with results of the simultaneous fit overlaid [3].

$$R_{\Xi_b^{*0}} = \frac{\sigma(pp \to \Xi_b^{*0}X)\,\mathcal{B}(\Xi_b^{*0} \to \Xi_b^- \pi^+)}{\sigma(pp \to \Xi_b^- X)}$$
$$= \frac{N(\Xi_b^{*0} \to \Xi_b^- \pi^+)}{N(\Xi_b^-)}\frac{\epsilon(\Xi_b^-)}{\epsilon(\Xi_b^{*0} \to \Xi_b^- \pi^+)} \quad (2)$$
$$= 0.23 \pm 0.02(\text{stat}) \pm 0.02(\text{syst}),$$

where N and ϵ refer to similar quantities as those in Eq. (1). The systematic uncertainties include variations for both Ξ_b^- and Ξ_b^{*0} fit model and again finite size of the MC simulation samples.

VI. OBSERVATION OF AN EXCITED BEAUTY STRANGE BARYON $\Xi_b(6100)^-$

The obtained $\Xi_b^- \pi^+ \pi^-$ invariant mass distribution is presented in Fig. 5, divided into the fully and partially reconstructed Ξ_b^- samples. A clear peak, corresponding to a signal of a new state, is observed near the kinematic threshold at a mass of 6100 MeV. No structures are seen

in the same sign $\Xi_b^- \pi^\pm \pi^\pm$ control samples, which are consistent with the combinatorial background of the opposite sign $\Xi_b^- \pi^+ \pi^-$ distributions.

Following analogues with the excited Ξ_c baryons, if the new state corresponds to the expected $1P$-excitation with $J^P = 3/2^-$, it should decay via $\Xi_b^{**} \to \Xi_b^{*0}\pi^- \to \Xi_b^-\pi^+\pi^-$, with the intermediate $\Xi_b^{*0} \to \Xi_b^-\pi^+$ transition. To account this feature, an additional mass window is applied on the $\Xi_b^-\pi^+$ mass to select the previously studied excited Ξ_b^{*0} baryon. The distributions of the invariant mass difference (same as previously described ΔM) in the signal region with the new selection requirement are presented in Fig. 6.

A simultaneous fit is performed to these distributions, with the signal modeled with a relativistic Breit–Wigner function convolved with a double-Gaussian resolution function (fixed from MC simulation), where mass and natural width of the resonance are shared between the two channels of the simultaneous fit. The background component is modeled with the threshold function $(\Delta M)^\alpha$. The results are also shown in Fig. 6.
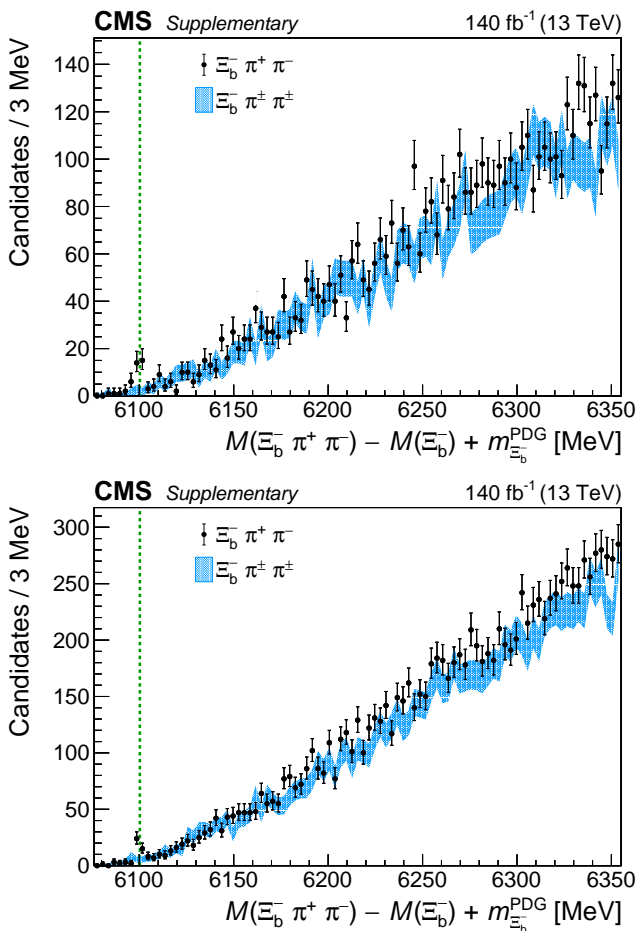
The local statistical significance of the peak ex-

FIG. 5: Invariant mass distribution of the selected $\Xi_b^- \pi\pi$ candidates for the opposite sign (circles) and same sign (band) events [2]. The Ξ_b^- ground state is fully reconstructed in the $J/\psi\Xi^-$ and $J/\psi\Lambda K^-$ channels (upper) or partially reconstructed in the $J/\psi\Sigma^0 K^-$ channel (lower). The vertical line shows the masses of the new $\Xi_b(6100)^-$ baryon.

FIG. 6: Distributions of the invariant mass difference $M(\Xi_b^- \pi^+ \pi^-) - M(\Xi_b^-) - 2m_{\pi^\pm}^{\rm PDG}$ for the selected $\Xi_b^- \pi^+ \pi^-$ candidates, with the Ξ_b^- reconstructed in the $J/\psi\Xi^-$ and $J/\psi\Lambda K^-$ channels (upper) or partially reconstructed in the $J/\psi\Sigma^0 K^-$ channel (lower) [2]. The result of the simultaneous fit is also shown.

ceeds 6 standard deviations. The mass difference of this state is measured to be $M(\Xi_b^- \pi^+ \pi^-) - M(\Xi_b^-) - 2m_{\pi^\pm}^{\rm PDG} = 24.14 \pm 0.22(\text{stat}) \pm 0.09(\text{syst})$ MeV, and using the known Ξ_b^- mass of 5797.0 ± 0.6 MeV [7] we obtain $M(\Xi_b(6100)^-) = 6100.3 \pm 0.2(\text{stat}) \pm 0.1(\text{syst}) \pm 0.6 (\Xi_b^-)$ MeV. The limited amount of data and present detector resolution do not allow us to measure the natural width of the new resonance, therefore an upper limit $\Gamma(\Xi_b(6100)^-) < 1.9$ MeV at 95% CL has been obtained through a scan of the profiled likelihood. The possible sources of the systematic uncertainties (included in both mass difference and natural width measurement) are similar to those previously described for Ξ_b^{*0} studies.

VII. CONCLUSIONS

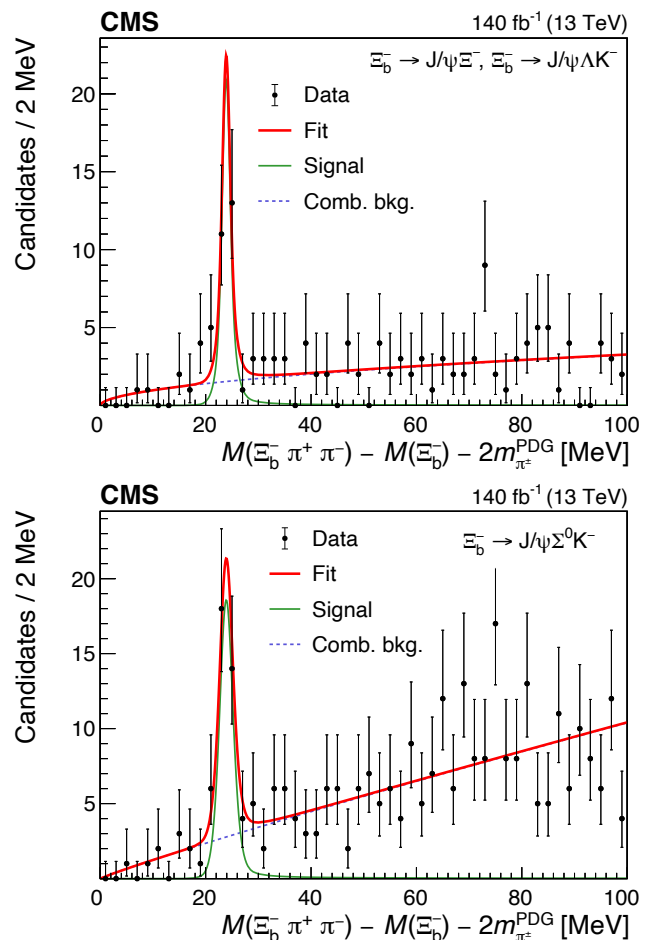The CMS Experiment is actively contributing to the heavy flavour physics, providing state-of-the-art spec-troscopy results. We report the first observation of the new $\Xi_b^- \to \psi(2S)\Xi^-$ decay together with its relative branching fraction to the $\Xi_b^- \to J/\psi\Xi^-$ decay [3]. We have also performed a study of the Ξ_b^{*0} baryon (also known as $\Xi_b(5945)^0$), providing the new measurements of its mass, natural width and the relative production w.r.t. the ground Ξ_b^- state [3]. Finally, new excited beauty strange baryon $\Xi_b(6100)^-$ is observed in $\Xi_b^- \pi^+ \pi^-$ invariant mass distribution. Its properties and decay sequence are consistent with being the lightest orbital excitation of Ξ_b^- baryon with spin-parity $J^P = 3/2^-$. Recently, this observation was confirmed by the LHCb Collaboration with high significance and precision [14].

All the presented results and measurements are clearly statistics-limited and suffer from large uncertainties. The nowadays ongoing Run-3 data-taking at the LHC is expected to collect more than a twice bigger dataset with the usage of new, inclusive dimion triggers, which should significantly improve the efficiency of Ξ_b topologies re-

construction, allowing us to perform new interesting spectroscopy studies.

to give the present talk and fruitful, exciting discussions during the Conference.

Acknowledgments

[1] S. Chatrchyan et al. (CMS), JINST **3**, S08004, 1 (2008).

[2] A. M. Sirunyan et al. (CMS), Phys. Rev. Lett. **126**, 252003 (2021), 2102.04524.

[3] A. Hayrapetyan et al. (CMS), Phys. Rev. D **110**, 012002 (2024), 2402.17738.

[4] S. Chatrchyan et al. (CMS), Phys. Rev. Lett. **108**, 252002 (2012).

[5] R. Aaij et al. (LHCb), JHEP **05**, 161 (2016).

[6] R. Aaij et al. (LHCb), Phys. Rev. Lett. **114**, 062004 (2015).

[7] R. L. Workman and others (Particle Data Group), PTEP **2022**, 083C01 (2022).

[8] R. Aaij et al. (LHCb), Phys. Rev. Lett. **121**, 072002 (2018).

[9] R. Aaij et al. (LHCb), Phys. Rev. D **103**, 012004 (2021), 2010.14485.

[10] R. Aaij et al. (LHCb), Phys. Rev. Lett. **128**, 162001 (2022), 2110.04497.

[11] A. G. Grozin, *Heavy quark effective theory* (Springer Berlin, Heidelberg, 2004).

[12] G. Punzi, in *Proceedings of PHYSTAT 2003, Statistical problems in particle physics, astrophysics and cosmology* (2003), p. MODT002, eConf C030908, physics/0308063.

[13] A. M. Sirunyan et al. (CMS), Phys. Lett. B **803**, 135345 (2020), 2001.06533.

[14] R. Aaij et al. (LHCb), Phys. Rev. Lett. **131**, 171901 (2023), 2307.13399.